Int. J. Electrochem. Sci., 7 **(2012)** 12668 - 12679

International Journal of
ELECTROCHEMICAL
SCIENCE
www.electrochemsci.org

Microstructure, Corrosion Resistance and Biocompatibility of Biomimetic HA-Based Ca-P Coatings on ZK60 Magnesium Alloy

Wei Lu[*], *Zhe Chen, Ping Huang and Biao Yan*

School of Materials Science and Engineering, Shanghai Key Lab. of D&A for Metal-Functional Materials, Tongji University, Shanghai 200092, China
[*]E-mail: : weilu@tongji.edu.cn

Received: 29 October 2012 / *Accepted:* 19 November 2012 / *Published:* 1 December 2012

Recently, magnesium alloys have attracted much attention as a metallic biodegradable implant because of their excellent biocompatibility and mechanical compatibility. However, magnesium has a poor corrosion resistance due to its active chemical properties, which limited the application in orthopedic surgery. In this work, Ca-deficit hydroxyapatite (HAp) coatings were prepared on the ZK60 magnesium alloys by a biomimetic method. The revised SBF solutions with pH value of 5~7 and Ca/P ratio of 1.67 were used. The coatings were composed of ball-like CaP particles with the Ca/P ratio of 0.86~1.24. Electrochemical corrosion, in vitro immersion and cytotoxic tests were conducted to evaluate the corrosion resistance and biocompatibility. The corrosion resistance and biocompatibility of the coated samples were greatly improved comparing with that of the uncoated sample. For the samples fabricated at different pH values, the sample coated from the solution with pH of 6 has the best corrosion resistance and biocompatibility.

Keywords: magnesium alloy; Ca-P coating; biomimetic method; corrosion; cytotoxicity

1. INTRODUCTION

Magnesium and its alloys have an excellent biocompatibility and mechanical compatibility as a biodegradable implant for human body. [1,2] Mg is an essential element for bone metabolism and may promote the formation of new bone tissue. In addition, the elastic modulus of Mg and its alloys is well-matched with that of natural bone, resulting in the reduction of the stress shielding effect that can lead to bone loss around the implant. It has the potential to be the alternative material for the traditional metal implants, which have good corrosion resistance, but poor biocompatibility and stress shielding effect, and need a second surgery to remove. [1,2] The degradable properties of Mg and its alloys are,

however, a double-edged sword. Magnesium and its alloys are very reactive and have a very high corrosion rate when immersed in physiological solutions, which are composed of organic acid, high concentration of chlorine ion and combined with proteins, enzymes and cells. And, the currently developed magnesium alloys degrade before the end of the bone healing process. In order for the use of Mg material to be feasible for orthopedic applications, there is a high demand to reduce the corrosion rate to meet the requirement of the synchronization between the implant biodegradation and the new bone formation by various surface treatment techniques.

Recently, the corrosion properties of Mg and its alloys have been investigated extensively [3~10] and a lots of studies have been performed for the purpose of reducing the corrosion rate of Mg, including alloying [11,12], processing [13,14] and protective coating [15~17]. Among them, coatings consisting of bioactive and biocompatible materials such as hydroxyapatite [$Ca_{10}(PO_4)_6(OH)_2$, HA] have been suggested as an effective means of reducing the corrosion rate and offering excellent biocompatibility additionally. Ideally, this would also minimize hydrogen production, which has been observed as a (potentially disadvantageous) corrosion byproduct when using this material.

Hydroxyapatite, the major composition of bone with excellent bioactivity and osteoconductivity, has been used as a coating on the traditional Ti alloys [18] and stainless steel [19] to improve the biocompatibility. Recently, some studies have been conducted to slow down the biodegradation rate of magnesium alloys by coating HA using chemical deposition, electrodeposition, hydrothermal treatment and alkali-heat treatment. [20] Though many methods for fabricating HA coatings are available, the biomimetic method [18, 21~23] offers the advantages of a simple, low temperature, non-toxic and non line-of-sight process. The technique is relatively simple to set up and perform, and is a cost-effective way of creating homogeneous coatings on several samples simultaneously and allows for complex shapes to be coated. The biomimetic coating process uses only ions found in the body fluids to create safe, biocompatible coatings with properties similar to natural bone.

Zinc is recognized as a highly essential element for humans. In zinc deficiency, nearly all the physiological functions are strongly perturbed. Zirconium possesses a set of suitable properties for orthopedic applications such as low specific weight, high corrosion resistance, and biocompatibility. Based on the above considerations, ZK60 magnesium alloy (Mg-5.5wt%Zn-0.5wt%Zr) was chosen in our studies. Biomimetic techniques used for HA-based CaP coating deposition are carried out in revised simulated body fluids (SBF), where HA phases are precipitated out of solution and ‘grown’ on the ZK60 substrate. The pH value of revised simulated body fluids is varied from 5 to 7 in order to refine fabricating protocols of HA-based CaP coatings. The microstructure and composition of the biomimetic HA-based CaP coatings were characterized, and the degradation properties and cytotoxicity were also investigated.

2. EXPERIMENTAL

2.1 Sample Preparation

The magnesium alloy used in this study was ZK60 alloy, with the major alloying elements of approximately 5.5wt% Zn and 0.5wt% Zr. It was cut into rectangular samples with a size of

$10\times10\times5mm^3$. These samples were ground with SiC papers up to 800#, rinsed ultrasonically in ethanol and then air dried. The dried samples were etched in phosphoric acid solution at 55℃, followed by neutralization in NaOH solution. Samples were then rinsed with distilled water and air dried.

2.2 Biomimetic HA-based CaP Coating

In this study, the Mg samples prepared earlier were applied with a layer of biomimetic Ca-P coating using a revised SBF. The ion concentrations of SBF and the revised SBF are listed in Table 1. These Ca and P concentrations were chosen to maintain the stoichiometric ratio of Ca/P in hydroxyapatite, 1.67:1, and several times as high as those of the SBF respectively. The initial pH of the revised solution was separately adjusted to 5, 6 and 7, using either hydrochloric acid or sodium hydroxide as required. The pre-treated Mg samples were immersed in the revised SBF with different pH for 7 days at ambient temperature. The samples were then removed from the solution, rinsed with deionized water, and dried in air.

Table 1. Composition of SBF and revised SBF solution

Component	Concentrations	
	Revised SBF(g/L)	SBF(g/L)
$CaCl_2$	0.333	0.1397
$MgSO_4$	0.09767	0.09767
KCl	0.4	0.4
KH_2PO_4	0.06	0.06
$NaHCO_3$	0.335	0.355
NaCl	8.0	8.0
$Na_2HPO_4\cdot12H_2O$	0.256	0.1206
D-Glucose	1.0	1.0

2.3 Surface Characterization

The crystallographic structure and chemical compositions of the coatings were examined using X-ray Diffraction (XRD) and energy dispersive spectroscopy (EDS), respectively. To study the morphology, coated samples were analyzed with a field emission scanning electron microscope (FE-SEM).

2.4 Electrochemical Measurements

Corrosion behavior of the samples was studied by Electrochemical tests (Tafel Plot) with a electrochemical work station. The experiments were performed in the SBF solution (listed in Table 1) with a pH value of 7.4 at 37 ℃. A three electrode set-up with a saturated calomel reference and a platinum counter electrode was used. The area of the samples for working electrode was $10\times10mm^2$.

Prior to characterization, the samples were immersed in the solution for 20 min to establish the open circuit potential.

2.5 Immersion Tests

Immersion tests were carried out in SBF solution. The pH value was adjusted to 7.4 ± 0.1 and the temperature was kept at 37 ± 0.5 ℃ using a water bath. The samples were immersed into 120 ml SBF solution for 8 days, respectively. The pH value of the solution and the samples' mass were recorded during the immersion every 24h, with a blank SBF solution as control group. The SEM characterizations were performed before and after immersion tests.

2.6 Cytotoxicity Tests

Murine fibroblast L-929 cell (purchased from cell bank of Chinese Academy of Sciences, Shanghai) was adopted to evaluate cytotoxicity. L-929 cells were cultured in Dulbecco's modified Eagle's medium (DMEM, high glucose), supplemented with 10% fetal bovine serum (FBS) in a humidified incubator at 95% relative humidity and 5% CO_2 at 37 ℃. The cytotoxicity tests were carried out by indirect contact. Extracts were prepared according to ISO 10993-5:1999. The extraction media were serially diluted to 25%, 50%, 75% and 100% concentration after 72h incubation at 37℃. Cells were incubated in 96-well flat bottomed cell culture plates at 1.5×10^4 cells ml^{-1} medium in each well and incubated for 24h to allow cell attachment. Then the medium was replaced by 100 μl extraction medium. After incubation in humidified atmosphere for 3 days, 20 μl MTT with a concentration of 5 mg/ml was added to each well and the samples were for 4h. Subsequently, 150 μl DMSO was added to each well and optical density (OD) measurements were conducted at a wavelength of 570nm.

3. RESULTS AND DISCUSSION

3.1 XRD Analysis

Figure 1 shows the XRD patterns of the samples with biomimetic CaP Coatings fabricated at different pH values. The XRD pattern of Mg substrate is also shown as comparison in Fig.1. It can be seen from Fig.1 that in the XRD spectrum of sample coated at pH=5, there is a relatively weak peak at around 2θ=26°, which is attributed to the (002) diffraction plane of HAp phase. In addition, a broad peak at 2θ=32°was observed in this spectrum, corresponding to overlapping of the (211) and (112) diffraction planes and indicative of a poorly crystalline, bone-like HAp. When the pH value of SBF solution is increased to 6, the peak at around 2θ=26° disappears and a new peak at about 2θ=26° which can be indexed as (203) plane of HAp, while the broad peak at 2θ=32°can still be observed in the XRD spectrum. When further increasing the pH value of SBF solution to pH=7, we can't find any peak of HAp phase but the only the peaks from Mg substrate can be observed in the XRD spectrum. But the

absence of HAp peaks in the XRD pattern does not mean that there is no CaP coating on the substrate. The reason may possibly be that the XRD signal from CaP coating in this sample is too weak.

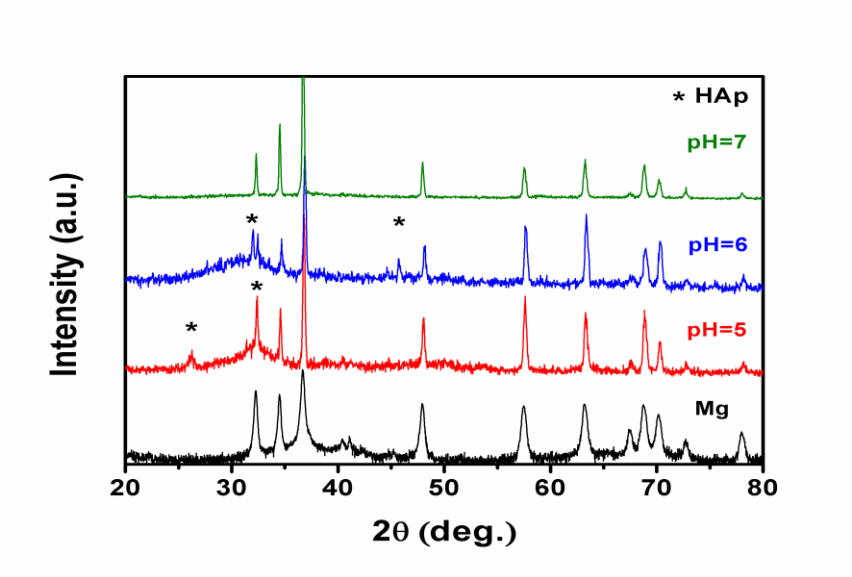

Figure 1.XRD patterns of Mg substrate and coated samples in different solutions with pH of 5, 6 and 7

3.2 Surface Morphologies and Compositions of the Ca-P Coatings

The biomimetic coating process designed for Ti was successfully applied to coat Mg substrates. The pH rise during the coating process decreased the solubility of the calcium and phosphate ions in solution, leading to heterogeneous nucleation of CaP on the substrate. The biomimetic coating process itself allowed deposition of a continuous CaP coating on the surface of the Mg substrates. Figure.2 presents surface morphologies and compositions of the coatings deposited from the revised SBF solution with the pH of 5, 6 and 7. SEM characterization reveals the differences between the morphology of the coatings formed at different pH values. Although the final coatings covered the substrates more or less uniformly on the macro scale, cracks and defects were observed in the coatings when observed under the SEM. From Fig.2 (a), it can be observed that the coating deposited at revised SBF solution with pH=5 has ball-like particles with a diameter of about 3~5μm, and a lot of ball-like particles stacked so closely that it showed dense cluster structure on the surface. For the coating deposited from the revised SBF solution with the pH of 6, it can be observed from Fig.2 (b) that the morphology of the coating is still of dense-cluster structure which is composed of ball-like particles with a diameter of about 1~4μm. Also, cracks are clearly observed in this sample. Fig.2 (c) depicts the coating morphology of the sample deposited at the pH of 7. The coating seems loose compared with the other two samples. A similar cluster-like morphology was observed in this sample. The clusters are composed of small particles which are not ball like as in the other two samples. And the diameters of the particle are very uniform and are in the range of around 1~2μm. In addition, pores were also observed among these tiny apatite clusters. Interestingly, the size of these particles decreased

substantially with the increasing pH values. An average apatite particle diameter of around 4, 2.5 and 1.5μm were observed for samples =5, 6 and 7, respectively.

The Ca/P ratio of the biomimetic coatings was examined by EDS to determine if the composition of biomimetic coating was similar to that of hydroxyapatite. The main elements detected on the surface of the film were Ca, P, C, and O, indicating that CaP was present in the coating. The calcium to phosphate ratio, as measured by EDS, was found to be around 1.24, 1.19 and 0.86 for coatings deposited at pH=5, 6 and 7, respectively, as shown in Fig.2. The Ca/P ratios of all the coatings are below that of the stoichiometric HAp (1.67). This is due to substitutions in the lattice. Calcium phosphate compounds can be substituted with different ions. In the HA lattice, calcium can be replaced by small amounts of magnesium and sodium, and phosphates can be replaced by carbonate ions [24]. During the biomimetic depositing process, these ions are incorporated into the coating. Mg is found to be present in significant quantities due to the revised SBF solution and the corrosion of the substrate during the coating process. This is mostly due to the presence of Mg^{+} and Cl^{-} ions in solution. The corrosion mechanism of magnesium in physiological fluid is strongly related to the presence of chloride ions, which destroy the passivation layer of $Mg(OH)_2$ [25~27]. Removing all of the chloride ions from the coating solutions may help to slow the corrosion, and limit the amount of Mg that makes its way into the coating. Substitution and interstitial Mg in the lattice affect the growth of the CaP crystal structure [28, 29]. The Mg present in the lattice inhibits the growth of crystalline apatite.

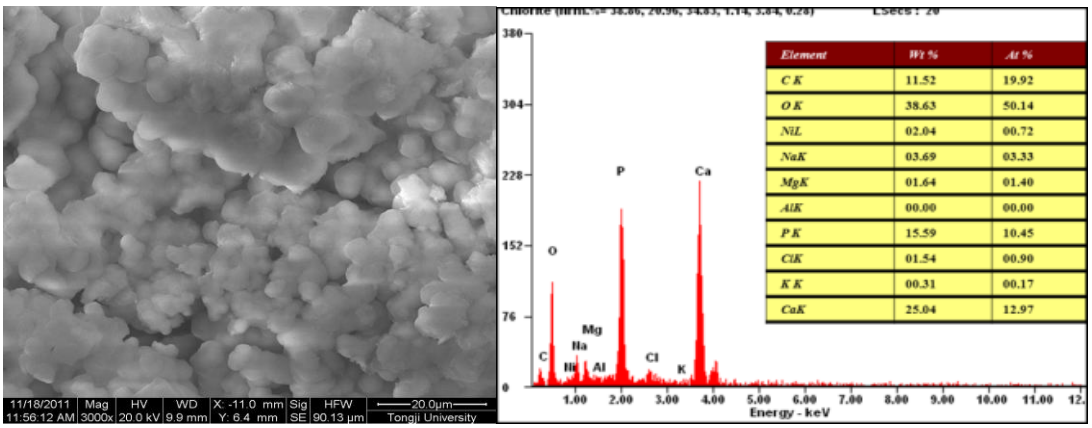

A D

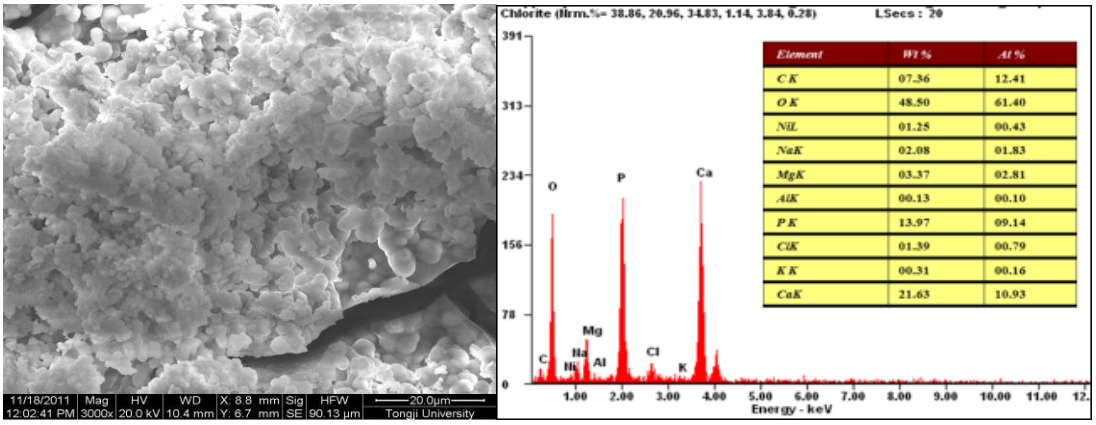

B E

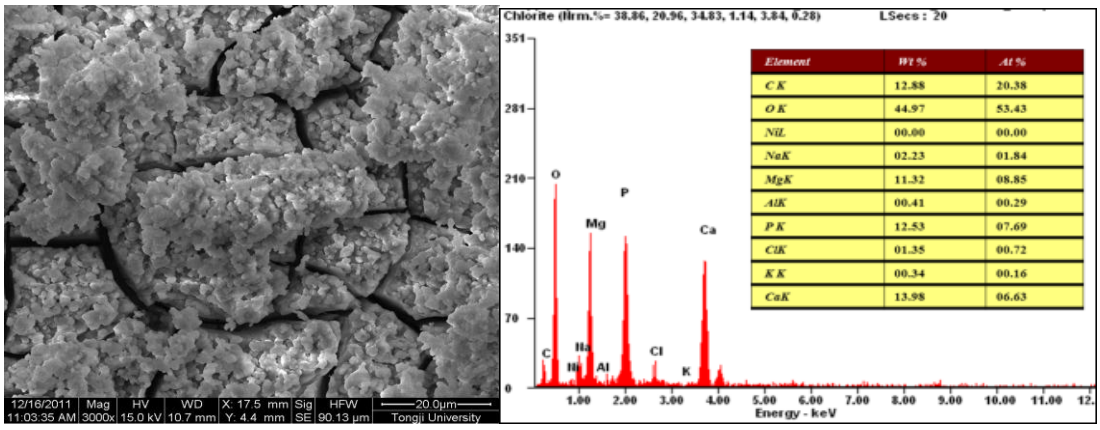

C F

Figure 2. SEM morphologies of coated samples (a)pH=5, (b)pH=6, (c)pH=7 and corresponding EDS of the coating (d) pH=5, (e) pH=6, (f) pH=7

3.3 Immersion tests in SBF

To evaluate the degradation behavior, the in vitro degradation behavior of the HA-coated and uncoated ZK60 alloy samples in SBF were monitored. The pH values of the SBF were monitored every day during the sample immersion. Figure.3 shows the variation of the pH value of SBF solution at different immersion time. The degradation rate of Mg alloys during the early stages of implantation would play a critical role in the initial surrounding tissue response. If the initial degradation of Mg-based implants was too rapid, osteolysis would occur, thus adversely affecting bone tissue regeneration.[30] Therefore, it was critical to control and decrease the initial degradation rate. From Fig.3, it can be seen that there is an increase in pH value for all the samples with increasing time. At the first day, the pH value increases sharply for all the samples because of the increase of OH^- concentration caused by the release of Mg^{2+} [31], but the pH for the uncoated sample reached the highest position, 9.0, while the pH is less than 8.6 for coated samples. After 8 days' immersion, the pH changes for all samples slow down. It is clear that the pH change for the uncoated sample was the highest, and the pH change of the solution immersed with the sample coated in solution with pH=6 slightly lower than that of the other samples. Therefore, it can be concluded that the samples coated with HAp have a better corrosion resistance than uncoated sample, and the sample coated in solution with pH=6 has the best corrosion resistance. The surface morphologies of the samples after immersion tests are showed in Figure 4. In Fig.4 (a), many cracks and white corrosion products can be observed in the uncoated sample. According to the EDS results (which are not shown here), the inner corrosion layer should be $Mg(OH)_2$, and the white corrosion products should be some Ca-P precipitates. In Fig.4 (b), (c), (d), the surface morphologies are almost the same. The surface is full of HA particles with some cracks caused by corrosions. It is obviously that there are fewer cracks in the sample coated in solution with pH=6 than the other samples. This is consistent with above results and the results of electrochemical characterization shown in next section.

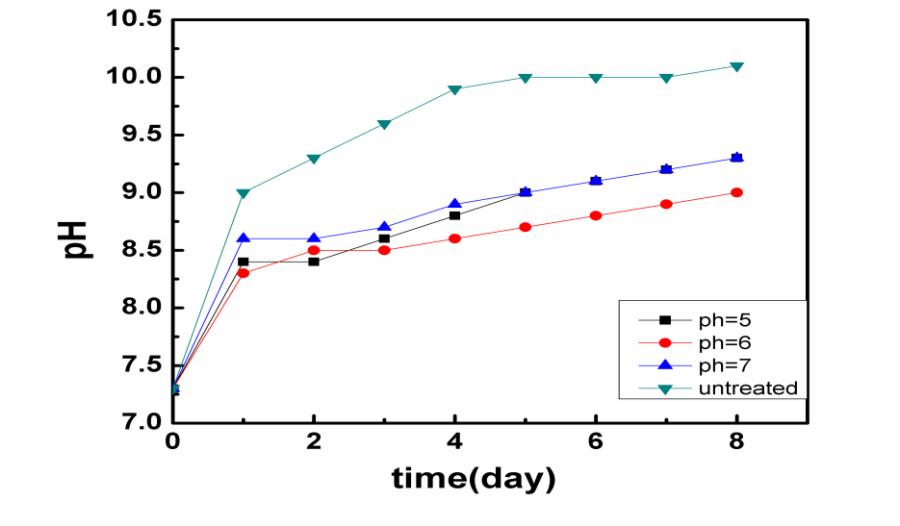

Figure 3. Variation of the pH values of SBF solution during immersion tests

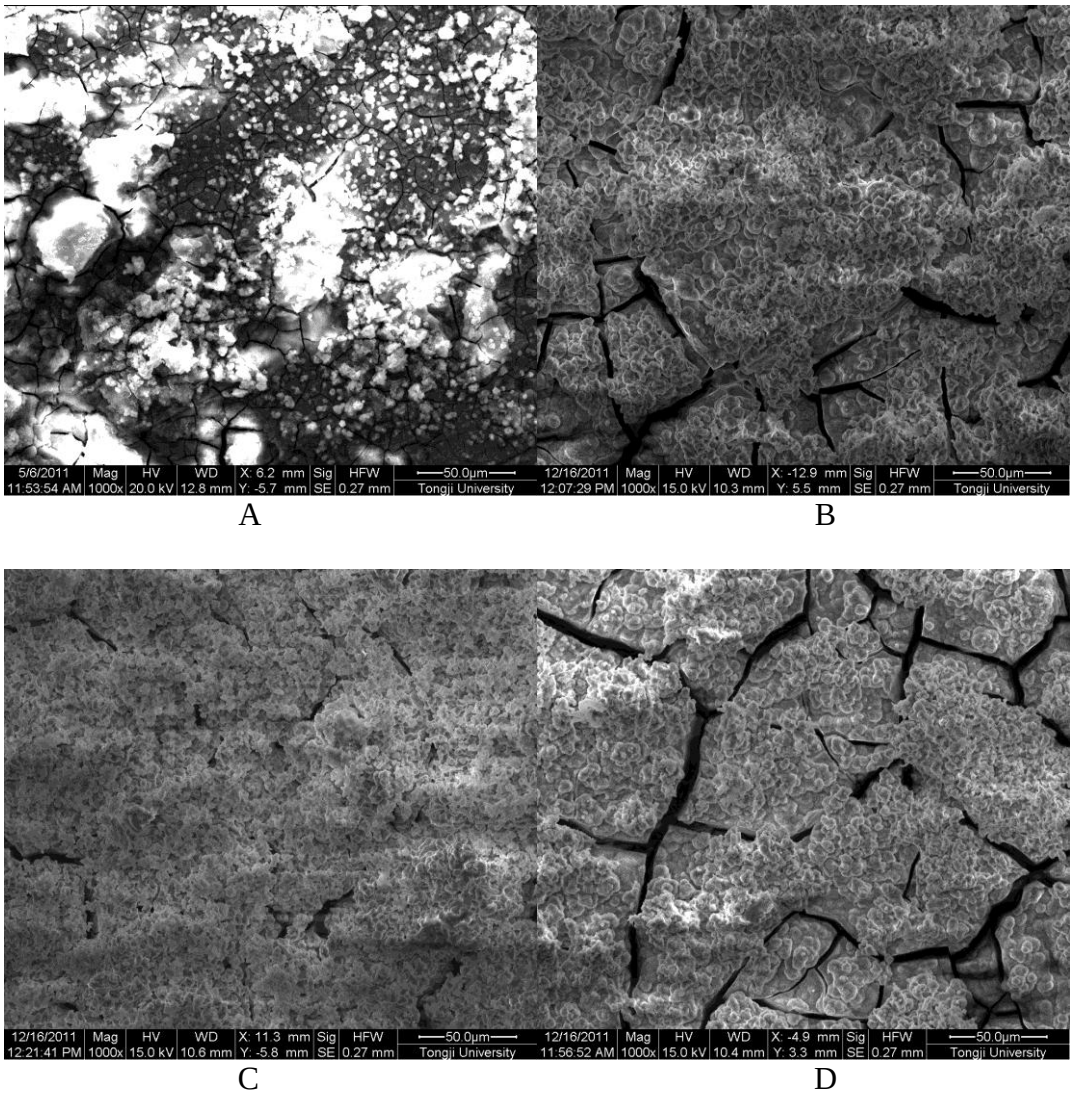

Figure 4. Morphologies of samples after immersion in SBF (a)uncoated (b)pH=5 (c)pH=6 (d)pH=7

3.4 Electrochemical Behavior in SBF

The polarization curves of the HA-coated and uncoated ZK61 alloy samples were plotted based on the electrochemical characterizations in SBF (Fig.5). The corrosion potential (E_{corr}) was determined according to Tafel extrapolation. Generally, a material that has a higher corrosion potential will have a lower degradation rate. The initial corrosion potential (E_{corr}) of the HA-coated Mg alloy samples were all higher than the uncoated alloy sample (-1.53V). The overall corrosion rate drops due to the calcium phosphate coating. The coating decreases the available surface area susceptible to corrosion. This matched with the immersion testing results that the initial degradation rate of the HA-coated samples was lower than the uncoated ones. Table.2 shows the electrochemical parameters of analyzed from Tafel curves. The coated samples have a better corrosion resistance than the uncoated sample, E_{corr} is improved by 120mV~180mV and I_{corr} decreased with about two order in magnitude. The corrosion potential of the sample coated at pH has the highest value of about -1.36V, indicating that this sample would be the least susceptible to degradation. It therefore makes sense that initially this coating will provide the greatest corrosion protection.

Table 2. Corrosion parameters obtained from electrochemical analysis

Samples	E_{corr} (V)	I_{corr} (A)
uncoated	-1.531	1.768e-004
pH=5	-1.377	4.467e-006
pH=6	-1.360	1.685e-006
pH=7	-1.417	9.450e-006

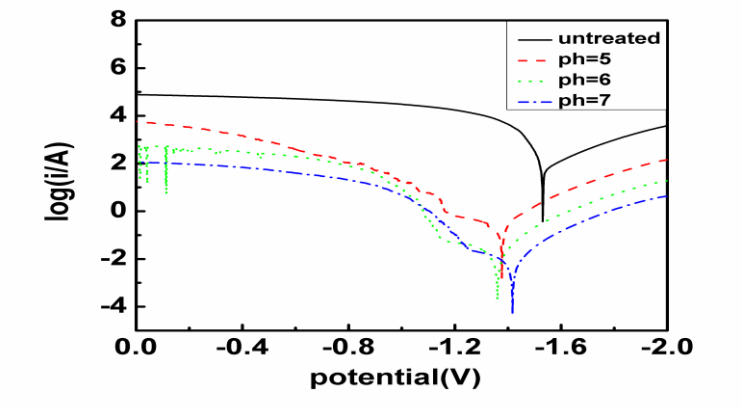

Figure 5. Tafel plot of the samples in SBF solution

3.5 Cytotoxicity

Figure.6 shows the L-929 cell viability cultured in the individual extraction mediums of samples with coatings deposited from the revised SBF solutions. After 3 days' culture, all absorption

values of coated samples were higher than that of the uncoated one. ANOVA tests [32] indicated that there were significant differences for uncoated sample and HAp-coated samples at the extract concentrations of 25%, 50%, 75%, 100% ($p<0.05$). It was seen that there was no significant difference for the coated samples deposited at different pH values at the extract concentrations of 25% ($p>0.05$). However, at the extract concentrations of 50%, 75% and 100%, there were significant differences ($p<0.05$). Especially at 50% and 75%, the differences were more notable ($p<0.01$).

For all the samples, it can be observed that the absorption value decreased with the increasing of the extract concentration. It explains that the amount of extract has an obvious influence on the viabilities of L-929 cells. At each concentration, the sample with coatings deposited from solution with the pH of 6 has the highest value.

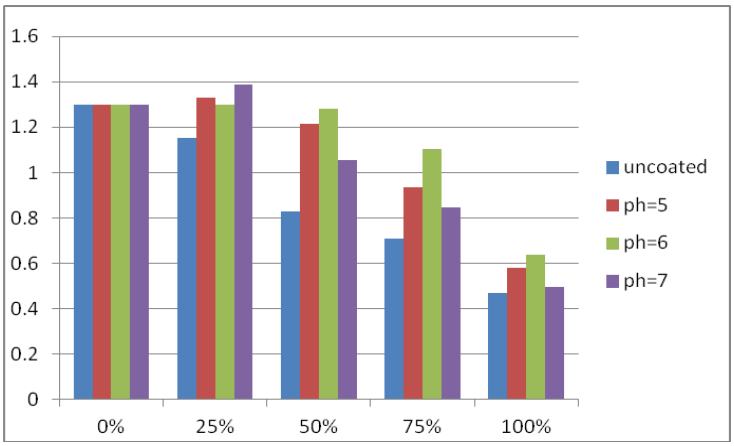

Figure 6. L-929 cell viability cultured in the individual extraction mediums of samples with coatings deposited from the revised SBF solutions (extract concentrations of 25%, 50%, 75%, 100% ($p<0.05$)).

Therefore, it can be concluded that the sample coated from solution with pH of 6 has the best cytocompatibility and the CaP coatings prepared by biomimetic method at different pH value of the solution can further improve the cytocompatibility of ZK60 alloy, whose cytotoxicity was also in a level of biosafety suitable for cellular applications.

4. CONCLUSIONS

In summary, Ca-P coating was successfully prepared on the ZK60 magnesium by a biomimetic method. The CaP coatings show a ball-like morphology and the Ca/P ratio is in the range of 0.86~1.24. The Ca-deficit HAp coating has tailored the corrosion of the magnesium substrate. The corrosion resistance of ZK60 alloy is obviously improved after coated with HAp coatings and the sample with HAp coating deposited from the solution with a pH of 6 has the best corrosion resistance. The cytotoxic tests showed the coated samples have good biocompatibility and the sample coated from the solution with a pH of 6 has the best biocompatibility.

ACKNOWLEDGEMENTS
The present work was supported by National Natural Science Foundation of China (Grant No. 50901052) and Program for Young Excellent Talents in Tongji University (Grant No. 2009KJ003) and "Chen Guang" project (Grant No.10CG21) supported by Shanghai Municipal Education Commission and Shanghai Education Development Foundation.

References

1. Mark P. Staiger, Alexis M. Pietak, Jerawala Huadmai, George Dias. *Biomaterials* 27 (2006) 1728–1734
2. Frank Witte, Norbert Hort, Carla Vogt, Smadar Cohen, Karl Ulrich Kainer,Regine Willumeit, Frank Feyerabend. *Current Opinion in Solid State and Materials Science* 12 (2008) 63–72
3. El-Sayed M. Sherif. *Int. J. Electrochem. Sci*., 7 (2012) 4235 – 4249
4. El-Sayed M. Sherif. *Int. J. Electrochem. Sci*., 7 (2012) 5084 – 5099
5. El-Sayed M. Sherif, Abdulhakim A. Almajid. *Int. J. Electrochem*. Sci., 6 (2011) 2131– 2148
6. S.M.M.Shanab, M. A.Ameer, A. M. Fekry, A. A. Ghoneim, and E. A. Shalaby. *Int. J. Electrochem. Sci.*, 6 (2011) 3017 – 3035
7. Zhan YU, Dongying JU, Hongyang ZHAO. *Int. J. Electrochem. Sci*., 7 (2012) 7098 – 7110
8. A.M. Fekry and M.A. Ameer. *Int. J. Electrochem. Sci*., 6 (2011) 1342 – 1354
9. Khalil Abdelrazek Khalil, El-Sayed M. Sherif, Abdulhakim A. Almajid. *Int. J. Electrochem. Sci*., 6 (2011) 6184 – 6199
10. W. Zhang, B. Tian, K. Q. Du, H. X. Zhang, F. H. Wang. *Int. J. Electrochem. Sci.*, 6 (2011) 5228-5248
11. Shanna Xu, Magdalene Edet Ikpi, Junhua Dong, Jie Wei, Wei Ke, Nan Chen. *Int. J. Electrochem. Sci.*, 7 (2012) 4735 – 4755
12. Hui Du, Zunjie Wei, Xinwang Liu, Erlin Zhang. *Materials Chemistry and Physics* 125 (2011) 568–575
13. Qiuming Peng, Shuangshuang Zhao, Hui Li, Ning Ma, Xuejun Li, Yongjun Tian. *Int. J. Electrochem. Sci.*, 7 (2012) 5581 – 5595
14. Xiaobo Zhang, Guangyin Yuan, Lin Mao, Jialin Niu, Penghuai Fu, Wenjiang Ding. *J. Mech. Behav. Biomed. Mater*., 7 (2012) 77-86
15. A. R. Shashikala, R.Umarani, S. M. Mayanna and A. K.Sharma. *Int. J. Electrochem. Sci*., 3 (2008) 993 – 1004
16. Jothi Sudagar, Guangli Bi, Zhonghao Jiang, Guangyu Li, Qing Jiang, Jianshe Lian. *Int. J. Electrochem. Sci*., 6 (2011) 2767 – 2788
17. JINGXIN YANG, FUZHAI CUI, and IN SEOP. LEE. *Annals of Biomedical Engineering*, 39, (2011) 1857–1871
18. Tal Reiner, Leonid M. Klinger, and Irena Gotman. Crystal Growth & Design, 11 (2011) 190-195
19. B. Bermúdez-Reyes, R. Puente-Ornelas, U. M. García-Pérez, P. Zambrano- Robledo, M. E. Contreras-García, J. Morales-Hernández, F. J. Espinoza-Beltrán. *Int. J. Electrochem. Sci*., 7 (2012) 2028 – 2035
20. Shaylin Shadanbaz, George J. Dias. *Acta Biomaterialia*, 8 (2012) 20–30
21. A. L. Oliveira, A. J. Pedro, C. Saiz Arroyo, J. F. Mano, G. Rodriguez, J. San Roman, R. L. Reis. *Journal of Biomedical Materials Research Part B: Applied Biomaterials*, 92B (2010) 55–67
22. F. Yang , J.G.C. Wolke, J.A. Jansen. *Chemical Engineering Journal* 137 (2008) 154–161
23. Ahmet Pasinli, Mithat Yuksel, Erdal Celik, Sevil Sener, A. Cuneyt Tas. *Acta Biomaterialia*, 6 (2010) 2282–2288
24. P. Habibovic, F. Barrere, C.A. Van Blitterswijk, K. De Groot, P. Layrolle, *Journal of the American* Ceramic Society 85 (2002) 517–522

25. G. Song, A. Atrens, *Advanced Engineering Materials* 5 (2003) 837–858
26. Y. Wang, M. Wei, J. Gao, J. Hu, Y. Zhang, *Materials Letters* 62 (2008) 2181–2184.
27. Y. Xin, K. Huo, H. Tao, G. Tang, P.K. Chu, *Acta Biomaterialia* 4 (2008) 2008–2015.
28. F. Barrere, Biomimetic Calcium Phosphate Coatings: Physicochemistry and Biological Activity , University of Twente, Enschede, 2002
29. A. Bigi, G. Falini, E. Foresti, A. Ripamonti, M. Gazzano, N. Roveri, *Journal of Inorganic Biochemistry* 49 (1993) 69–78.
30. R.–G. Guan, I. Johnson, T. Cui, T. Zhao, Z.-Y. Zhao, X. Li, H. Liu, *J. Biomed Mater Res A.*, 100 (2012) 999-1015
31. A. Atrens, M. Liu, N. I. Z.l Abidin, *Materials Science and Engineering B*, 176 (2011) 1609-1636
32. Z. Li, X. Gu, S. Lou, Y. Zheng, *Biomaterials*, 29 (2008) 1329-1344